Filamin A Stabilizes FcγRI Surface Expression and Prevents Its Lysosomal Routing[1]

Jeffrey M. Beekman,[2]* Cees E. van der Poel,[2]* Joke A. van der Linden,* Debbie L. C. van den Berg,* Peter V. E. van den Berghe,* Jan G. J. van de Winkel,*† and Jeanette H. W. Leusen[3]*

Filamin A, or actin-binding protein 280, is a ubiquitously expressed cytosolic protein that interacts with intracellular domains of multiple receptors to control their subcellular distribution, and signaling capacity. In this study, we document interaction between FcγRI, a high-affinity IgG receptor, and filamin A by yeast two-hybrid techniques and coimmunoprecipitation. Both proteins colocalized at the plasma membrane in monocytes, but dissociated upon FcγRI triggering. The filamin-deficient cell line M2 and a filamin-reconstituted M2 subclone (A7), were used to further study FcγRI-filamin interactions. FcγRI transfection in A7 cells with filamin resulted in high plasma membrane expression levels. In filamin-deficient M2 cells and in filamin RNA-interference studies, FcγRI surface expression was consistently reduced. FcγRI localized to LAMP-1-positive vesicles in the absence of filamin as shown by confocal microscopy indicative for lysosomal localization. Mouse IgG2a capture experiments suggested a transient membrane expression of FcγRI before being transported to the lysosomes. These data support a pivotal role for filamin in FcγRI surface expression via retention of FcγRI from a default lysosomal pathway. *The Journal of Immunology,* **2008, 180: 3938–3945.**

Immune cells interact with Ab-Ag complexes through a variety of FcR (1). The class I IgG receptor (FcγRI) is constitutively expressed on monocytes, macrophages, and dendritic cells. FcγRI is a high-affinity receptor for IgG and exists as a multimeric complex comprised of a ligand-binding α-chain and the FcR γ-chain (2–4). Its in vivo role is illustrated by FcγRI$^{-/-}$ mice that exhibit impaired Ab-dependent cellular processes such as bacterial clearance, phagocytosis, Ag presentation, and cytokine production (5, 6). For signaling, FcγRI relies both on the FcR γ-chain and the cytosolic domain of its α-chain (FcγRI-CY (cytoplasmic tail)[4]). FcγRI-CY facilitates MHC class II Ag presentation without active FcR γ-chain signaling (7), whereas deletion of FcγRI-CY retarded kinetics of endocytosis and phagocytosis, and abrogated FcγRI-triggered IL-6 secretion (8). Unlike the FcR γ-chain, FcγRI-CY does not contain ITAM or other tyrosine-containing signaling motifs.

Identification of interacting partners of FcγRI-CY may aid in deciphering signaling routes that control FcγRI function. We recently described an interaction between FcγRI-CY and periplakin that affects FcγRI-ligand binding, and downstream effector functions (9, 10). Previously, actin-binding protein 280, or filamin A (filamin), was shown to coimmunoprecipitate with FcγRI (11). Filamin represents a homodimer composed of 280-kDa subunits that organizes actin filaments into orthogonal networks (reviewed in Refs. 12 and 13). In this study, we identified filamin in yeast two-hybrid screens using FcγRI-CY, and functionally characterized this interaction. Studies with a naturally filamin-deficient cell line (M2 cells), and a filamin-reconstituted subclone (A7 cells) indicated filamin to be crucial for cell morphology and locomotion, as well as subcellular localization and signaling of various receptors (14–21). To address the role of filamin for FcγRI biology, the subcellular distribution of FcγRI and filamin was studied in human monocytes. Stable FcγRI transfectants were generated in filamin-deficient M2 cells, and its filamin-reconstituted subclone A7, to assess the biological role of FcγRI-filamin interaction.

Materials and Methods

Constructs and chemicals

FcγRI (Gen Bank accession number L03418) was subcloned from pcDNA3 (22) (Invitrogen Life Technologies) containing neomycin resistance to pcDNA3.1 with zeocin resistance. The murine FcR γ-chain was *Hin*dIII/*Xba*I cloned into pCB7 containing hygromycin resistance (22). The TCR α-chain of pMX-TCRα-chain-internal ribosomal entry site-GFP (23), provided by Dr. S. B. Ebeling (Department of Hematology, University Medical Center, Utrecht, The Netherlands), was removed by *Bam*HI/*Not*I digestion and replaced by FcγRI or FcαRI subcloned from pCAV (24). PCR reagents for cloning were from PerkinElmer except for oligonucleotide primers (Isogen Bioscience). All constructs were verified by dideoxy sequencing using BigDye Terminators (Applied Biosystems) and analyzed on an ABI Prism 3100 Genetic Analyzer (Applied Biosystems). Chemicals were obtained from Sigma-Aldrich, unless stated otherwise.

Yeast two-hybrid screens

A MATCHMAKER human bone marrow cDNA library from BD Clontech was screened with FcγRI-CY as described in Ref. 22. Protein interactions were assessed by growth of transfected yeast cells on selective medium lacking leucine, tryptophane, and histidine, and a filter-lift β-galactosidase assay.

Cell culture, transfection, and bafilomycin A1 treatment

Human peripheral blood monocytes were isolated from healthy volunteers. Mononuclear cells were isolated from Ficoll gradients, and cultured with

*Immunotherapy Laboratory, Department of Immunology, University Medical Center, and †Genmab, Utrecht, The Netherlands

Received for publication April 27, 2006. Accepted for publication January 15, 2008.

The costs of publication of this article were defrayed in part by the payment of page charges. This article must therefore be hereby marked *advertisement* in accordance with 18 U.S.C. Section 1734 solely to indicate this fact.

[1] This work was supported by Medarex Europe (to J.M.B.) and Dutch Science Foundation Grant NWO/ALW 07764 (to C.E.v.d.P.).

[2] J.M.B. and C.E.v.d.P. contributed equally to this manuscript.

[3] Address correspondence and reprint requests to Dr. Jeanette H. W. Leusen, Department of Immunology, University Medical Center, Lundlaan 6, Utrecht, 3584 EA, The Netherlands. E-mail address: J.H.W.Leusen@umcutrecht.nl

[4] Abbreviations used in this paper: CY, cytoplasmic tail; siRNA, short interfering RNA; NP40, Nonidet P-40; ER, endoplasmatic reticulum; EEA-1, early endosomal Ag-1; LAMP, lysosomal-associated membrane protein.

Copyright © 2008 by The American Association of Immunologists, Inc. 0022-1767/08/$2.00

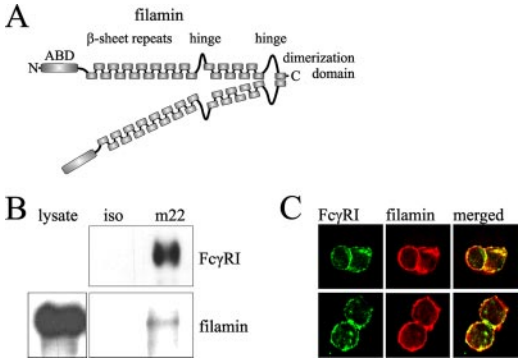

FIGURE 1. FcγRI interaction with filamin in yeast cells. *A*, Schematic representation of filamin; ABD, actin-binding domain. *B*, Coimmunoprecipitation of filamin and FcγRI. U937 cells were lysed after overnight stimulation with IFN-γ. Subsequently, immunoprecipitation was performed using an anti-FcγRI Ab (m22) or isotype control (iso). Western blotting was used to detect immunoprecipitated FcγRI (*top panel*) and coimmunoprecipitated filamin (*lower panel*). Experiments were performed three times, all yielding similar data. *C*, Subcellular localization of FcγRI and filamin in monocytes. Cells were stimulated overnight with 300 U/ml IFN-γ. Cells were adhered to glass slides, fixed in methanol, and FcγRI was stained with CD64 mAb H22 conjugated to FITC. Filamin was stained red. Green, red, and merged pictures of two stainings are shown. Colocalization is indicated in yellow.

IMDM containing L-glutamine (Invitrogen Life Technologies) supplemented with 10% FCS, penicillin, and streptomycin. After ~3 h at 37°C, nonadherent cells were removed, and adherent cells were incubated overnight with 300 IU/ml IFN-γ (IFN-γ1b; Boehringer Ingelheim). Human melanoma cells selected for filamin deficiency (M2) and its filamin reconstituted subclone (A7) were cultured as described (14). Cells were transfected with fugene (Roche) according to the manufacturer's instructions. Stable FcγRI-transfected cells were selected with zeocin (500 μg/ml). Inhibition of lysosomal maturation was accomplished by incubating cells with 100 nM bafilomycin A1 in medium for various time points. Carrier control represents DMSO 500-fold diluted in medium. U937 cells were cultured in RPMI 1640 (Invitrogen Life Technologies) supplemented with 10% FCS, 100 U/ml penicillin (Invitrogen Life Technologies), and 100 μg/ml streptomycin (Invitrogen Life Technologies).

Immunoprecipitation

For FcγRI immunoprecipitation, U937 cells were stimulated with IFN-γ overnight. Cells were then lysed in cold Nonidet P-40 (NP40) buffer, 1% NP40 in PBS solution with Complete EDTA-free protein inhibitor mixture (Roche). Lysates were incubated overnight with either isotype control (Sigma-Aldrich) or m22 Abs (Medarex Europe) coupled to protein A/G beads (Santa Cruz Biotechnology). Subsequently, beads were washed in NP40 buffer, boiled in sample buffer, and subjected to Western blotting.

RNA interference

U937 cells were transfected with siGenome SMARTpool targeting human filamin A or with nontargeting siControl smartpool (Dharmacon) using Amaxa nucleofection. Cells were cultured in RPMI 1640 10% FCS and stimulated overnight with IFN-γ after 48 h. Seventy-two hours posttransfection, when filamin knockdown was maximal, the cells were stained with mAb anti-CD64 M22-FITC (Medarex) and analyzed on a FACSCalibur (BD Biosciences). Filamin protein levels were assessed by Western blotting using mAb1680 anti-human filamin A (Chemicon International) followed by goat anti-mouse IgG-HRP (Jackson ImmunoResearch Laboratories). For flow cytometric analysis of filamin protein levels, cells were fixed with 4% paraformaldehyde and stained in PBS containing 0.1% BSA, 0.1% saponin, 5% goat serum, and 5% rabbit serum using mAb 1680 and goat anti-mouse IgG-RPE (Southern Biotechnology Associates).

Capture experiments using mIgG2a-FITC

M2 or A7 stabile transfectants were incubated with 2 μg/ml mouse IgG2a-FITC (DakoCytomation) in RPMI 1640 10% FCS at 37°C or at 4°C. After 6 h, cells were washed with PBS and trypsinized. Subsequently, cells were split and washed three times with either normal RPMI 1640 2% FCS or with RPMI 1640 2% FCS adjusted to pH 2.5 (acidic wash) (25). Cells were then analyzed using a FACSCalibur (BD Biosciences).

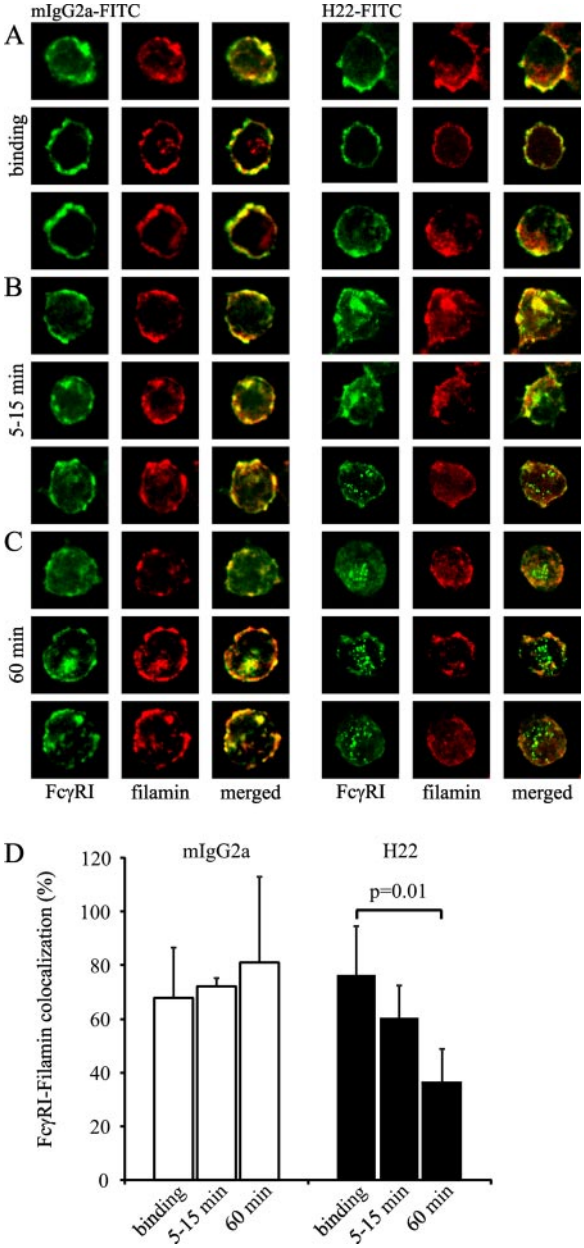

FIGURE 2. Subcellular localization of FcγRI and filamin in IFN-γ-stimulated monocytes. *A*, Monocytes were stimulated overnight with 300 U/ml IFN-γ. Cells were incubated with monomeric mIgG2a or mAb H22 (both FITC-conjugated) for 60 min at 4°C. Cells were then fixed, and stained for filamin. Three representative cells are shown. *B* and *C*, FcγRI ligands were added at 37°C at $t = 0$, and remained present throughout the experiment. Cells were fixed at different time points (*B*: 5–15 min, *C*: 60 min, three representative examples shown). Filamin was stained red. Experiments were repeated three times, all yielding similar data. *D*, The amount of FcγRI/filamin colocalization was quantified using Image J (see *Materials and Methods*), and the percentage of FcγRI/filamin colocalization was expressed as function of time ($n = 4$, Student's t test); 100% colocalization was determined by incubating H22-FITC or mIgG2A for 60 min at 4°C. Error bars indicate SD.

Immunofluorescence

Monocytes were isolated as described above, resuspended in PBS with 2 mM EDTA and 0.1% BSA, washed in medium, and adhered to poly-L-lysine-coated object glasses. For costainings with filamin, cells were fixed

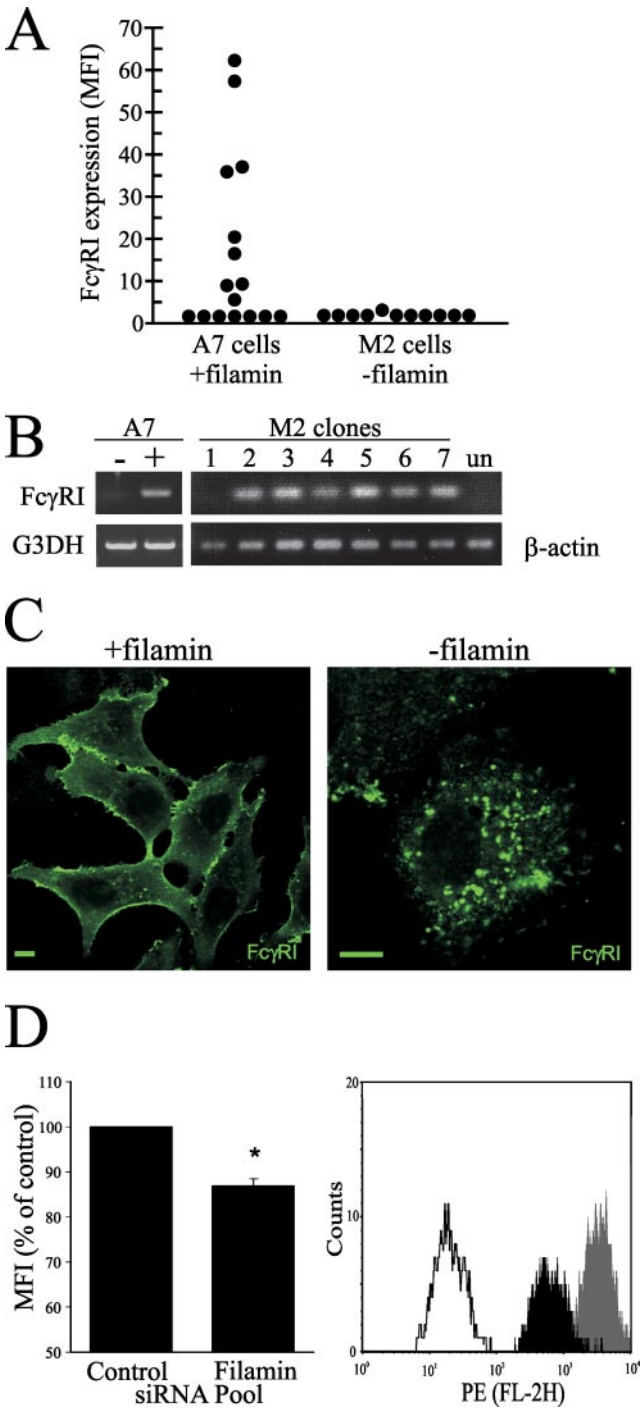

FIGURE 3. FcγRI surface expression on cells with or without filamin. *A*, Stable zeocin-resistant clones were randomly selected from three independent transfection experiments in cells with or without filamin. FcγRI expression was detected by CD64 mAb 10.1-FITC, and assessed by flow cytometry. Mean fluorescence intensities (MFI) are indicated. *B*, RNA was extracted from two A7 clones (*left lane* negative (−), and *right lane* positive (+) for FcγRI surface expression) and seven M2 clones, and RT-PCR for FcγRI was performed. *C*, Subcellular localization of FcγRI in filamin-deficient and filamin-reconstituted cells. FcγRI was stained by monoclonal 10.1-FITC after paraformaldehyde fixation (4) in filamin expressing clones (*left panel*) and filamin-deficient M2 cells (*right panel*). Bar marks 20 μm. *D*, Relative FcγRI surface expression after filamin knockdown in U937 cells using siRNA (nontargeting control pool vs filamin targeting pool) was assessed by flow cytometry (*left panel*, ∗, $p = 0.004$, Mann-Whitney test, $n = 3$). Error bars indicate SD. Filamin knockdown was confirmed by Western blot (data not shown) and flow cytometry (*right panel*, one representative experiment). Open histogram depicts background of secondary Ab; gray histogram depicts filamin staining in cells transfected with control pool; and black histogram shows cells transfected with filamin targeting pool.

in methanol at −20°C, washed extensively, and permeabilized in PBS containing 0.1% saponin, 0.2% BSA, 5% normal goat serum, and 5% normal rabbit serum. FcγRI was stained with 10 μg/ml FITC-conjugated humanized anti-FcγRI mAb H22 (Medarex). Filamin was stained by mIgG1 anti-filamin (Chemicon International), and goat anti-mIgG1-Alexa 555 conjugates (Molecular Probes). For internalization experiments, adhered cells were incubated in medium with 10 μg/ml FITC-conjugated H22 or mIgG2a for various time points at 37°C, fixed with methanol, and stained for filamin. Melanoma cells were grown on coverslips, fixed in PBS with 3% paraformaldehyde (or methanol when filamin was costained), and stained for FcγRI as described above, or with H22 $F(ab')_2$ followed by FITC-conjugated goat $F(ab')_2$ anti-human-κ-L chain (Southern Biotechnology Associates). Endoplasmatic reticulum (ER) was indicated by rabbit anti-calreticulin, *cis*-Golgi by anti-GM130, and *trans*-Golgi by anti-p230; endosomal and lysosomal compartments were indicated with anti-early endosomal Ag-1 (EEA-1), anti-CD63, and anti-CD107a (all mIgG1 unless indicated otherwise; BD Biosciences). Secondary detection was with goat anti-mIgG1-Alexa 555 conjugates (Molecular Probes), or goat anti-rabbit CY3 conjugates (Jackson ImmunoResearch Laboratories). For transferrin internalization, cells were incubated with 40 μg/ml transferrin conjugated to Alexa 555 (Molecular Probes) at 4°C, washed, and incubated at 37°C in medium for 15 min, fixed and processed for immunofluorescence as above. Slides were examined with a ×63 planapo objective on a Leitz DMIRB fluorescence microscope (Leica) interfaced with a Leica TCS4D confocal laser microscope. Colocalization was quantified with Image J (http://rsb.info.nih.gov/ij/) using identical settings for each experiment (minimal pixel threshold 50, ratio 50%). Images from total cells were assessed for pixels that were positive both in the green (FcγRI) and red channel (subcellular markers, or filamin) and the total number of pixels in the green channel (FcγRI). The percentage of FcγRI colocalization with subcellular marker/filamin = colocalized pixels between FcγRI and a specific marker/total FcγRI pixels × 100%.

Flow cytometry

M2 and A7 cells were detached 48 h posttransfection, and stained in PBS containing 0.1% BSA, 2 mM EDTA, and 10% normal mouse serum. Cells were washed, and surface FcγRI, or total FcγRI was detected with mAb 10.1-FITC (Serotec) in the absence or presence of 0.1% saponin, respectively, at 4°C. Cells were washed and analyzed with a FACSCalibur (BD Biosciences). Surface expression was scored positive when it exceeded three times background staining of untransfected cells. When FcγRI expression was compared with FcαRI expression, FcγRI and FcαRI were stained in 40 μl with 20 μg/ml mIgG1 clone 10.1 and A59, respectively, followed by 10 μg/ml goat anti-mouse PE conjugated (Jackson ImmunoResearch Laboratories).

RT-PCR

RNA was extracted from cells with Qiagen RNeasy midi columns (Qiagen), and reverse transcribed with oligo-dT primers of a GeneAmp RNA PCR kit (Applied Biosystems). FcγRI was amplified by 33 cycles as described in Ref. 22. Actin was amplified by 25 cycles with 5′-gtggggcgc ccccaggcaccag-3′ and 5′-ctccttaatgtcacgcacgatttc-3′ under standard conditions for PCR.

Western blot

A total of 1×10^5 cells were lysed in reducing Laemmli sample buffer, and proteins were separated with SDS-PAGE (12% gel). Proteins were transferred to nylon membranes, and stained for FcR γ-chain (Upstate Biotechnology) that was detected by goat anti-rabbit conjugated to HRP (Pierce). ECL and Biomax films were obtained from Amersham Biosciences.

Results

Filamin interacts directly with cytoplasmic domains of multiple receptors, and can profoundly affect their function (13). We found filamin (a schematic representation of filamin is shown in Fig. 1*A*) to interact with FcγRI using yeast two-hybrid screens on a bone marrow cDNA library. Cotransfection of the filamin-containing cDNA with empty bait plasmids did not allow yeast cells to grow

on selective medium (data not shown). Importantly, we confirmed this interaction by coimmunoprecipitating filamin via FcγRI from IFN-γ-stimulated U937 cells expressing both proteins endogenously (Fig. 1*B*). We next analyzed the subcellular localization of FcγRI and filamin in primary IFN-γ-stimulated monocytes (Fig. 1*C*). A significant portion of FcγRI and filamin colocalized at the plasma membrane when cells were fixed and stained with the CD64 mAb H22.

When monocytes were incubated with monomeric ligand (mIgG2a-FITC), or cross-linking FcγRI mAb (H22-FITC) that can trigger FcγRI internalization (26, 27), extensive colocalization was observed at the plasma membrane, and on mIgG2a-positive intracellular compartments (Fig. 2, *A–C*, *left panels*). Some filamin still colocalizes intracellularly with FcγRI at early time points (5–15 min) after H22-FITC incubation (Fig. 2, *A* and *B*, *right panels*). However, H22-FITC induced drastic FcγRI-filamin dissociation at later time points (Fig. 2, *A–C*, *right panels*, and *D*). Together, these results suggest that FcγRI and filamin predominantly interact at the plasma membrane, and to a minor extent at an intracellular compartment.

Next, we studied FcγRI in a filamin-deficient cell system, and stably transfected filamin-deficient M2 cells, and its filamin-reconstituted subclone A7 with the α-chain of FcγRI (FcγRI) (14). From three independent FcγRI transfections, 16 zeocin-resistant A7 clones and 12 M2 clones were selected. FcγRI surface expression in A7 cells was observed in ~50% of subclones (8 of 16 clones; Fig. 3*A*). Surprisingly, FcγRI cell surface expression in 12 subcloned M2 cells was extremely low or even undetectable, albeit six of seven M2 transfectants expressed FcγRI at the transcript level (Fig. 3*B*). This indicated filamin to be an important determinant of FcγRI surface expression (percentage FcγRI-positive A7 clones were compared with M2 clones, Fisher's exact test $p = 0.0083$). Next, we assessed FcγRI expression at the subcellular level in A7 and M2 cells by confocal microscopy (Fig. 3*C*). In the presence of filamin, FcγRI surface expression was evident, although some intracellular staining could be detected. In M2 cells lacking filamin, FcγRI-specific staining predominantly localized intracellularly, and was more difficult to detect suggesting lower total FcγRI protein levels (Fig. 3*C* (and see Fig. 7*A*)). M2 cells were confirmed to be filamin negative by Western blot and immunofluorescence analyses (data not shown). FcγRI colocalized with filamin at the plasma membrane, and to some extent at intracellular vesicles in A7 cells (data not shown; $n = 3$). Knockdown of filamin using short interfering RNA (siRNA) in U937 cells lead to a decreased cell surface expression of endogenous expressed FcγRI (Fig. 3*D*, *left panel*; Mann-Whitney *U* test, $p = 0.004$). Filamin knockdown was confirmed by flow cytometry (Fig. 3*D*, *right panel*) and Western blot (data not shown).

To assess whether the defective plasma membrane expression in M2 cells was selective for FcγRI, we included the receptor for IgA—FcαRI or CD89—as a control in transient transfections of M2 cells and A7 cells with FcγRI. Both receptors were expressed from vectors that coexpressed enhanced GFP. Surface expression levels of FcγRI, and FcαRI were comparable upon transfection in cells with filamin (Fig. 4*A*, $n = 3$). Transfection efficiencies were comparable as indicated by GFP signals. Cells without filamin, however, displayed impaired FcγRI surface levels, whereas FcαRI surface levels were unaffected. Control staining was performed on mock GFP-transfected cells with isotype controls (Fig. 4*A*) and untransfected cells (data not shown, $n = 3$). Similar differences were apparent at days 3 and 4 posttransfection (data not shown, $n = 2$).

In mice, in vivo surface expression of many FcR, including FcγRI, has been found to (partly) rely on the associated FcR

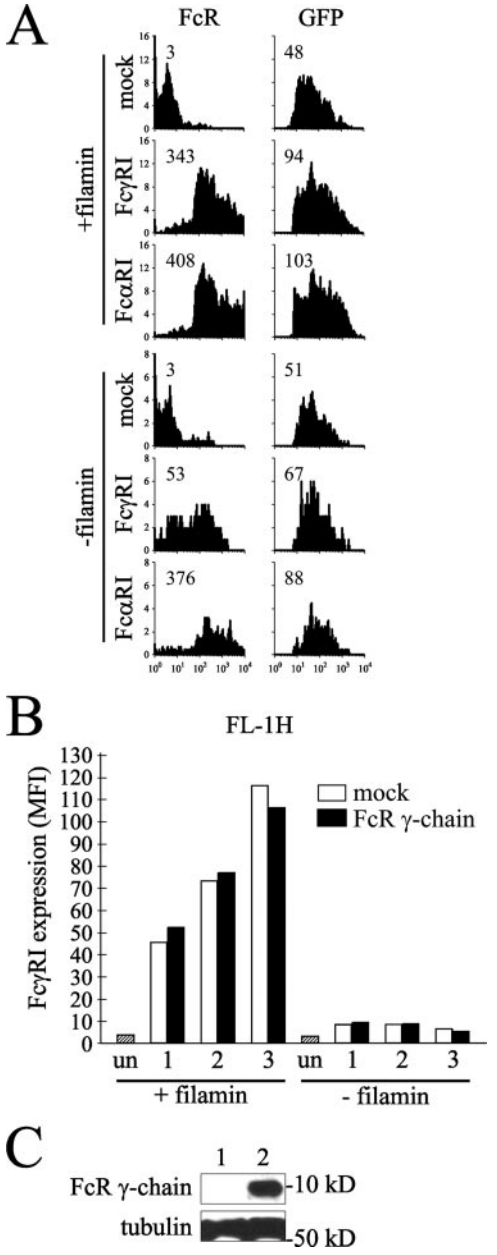

FIGURE 4. *A*, Transient transfection of M2 and A7 cells with FcγRI and FcαRI cDNA. Cells were transfected with FcγRI, and FcαRI expressed from plasmids that coexpressed enhanced GFP. FcγRI and FcαRI were stained with mAb M22 and A59, respectively, followed by incubation with PE-labeled anti-mouse IgG and flow cytometry. Gates for viable GFP-positive cells were applied, and cells were assessed for FcR and GFP expression 48 h posttransfection. Histograms of GFP-gated cells stained for FcγRI and FcαRI are shown in the *left column*, associated GFP levels are shown on the *right.* Cells were transfected with the original vector that coexpressed TCR α-chain and GFP to check for staining specificity. The mock cells shown in this figure were transfected with the original vector that coexpressed TCR α-chain and GFP and stained with Abs against FcγRI. However, essentially the same results were obtained when these cells were stained with Abs against FcαRI (data not shown). MFI are shown in the *top left corner* of each histogram. Three experiments were performed, yielding essentially identical results. *B*, Effect of FcR γ-chain transfection on FcγRI surface expression. Three filamin-positive and filamin-negative lines that expressed FcγRI transcripts were transfected with FcR γ-chain (■) or mock plasmid (□). ▨, Untransfected parental cells (un). Cells were stained for surface FcγRI by mAb 10.1-FITC and assessed by flow cytometry (MFI are indicated). Two experiments yielded similar data. *C*, Western blot for FcR γ-chain, and tubulin after transfection of mock (*lane 1*) or FcR γ-chain (*lane 2*) plasmids in M2 cells. Transfected A7 cells showed similar levels of FcR γ-chain. Tubulin was used as loading control.

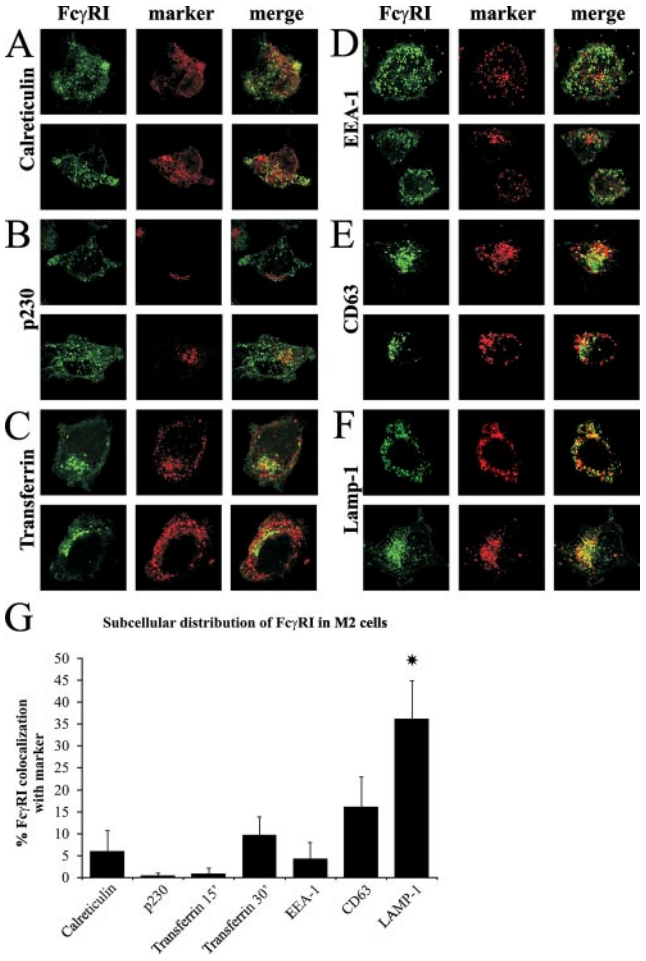

FIGURE 5. Intracellular location of FcγRI in cells without filamin. M2 cells were stained for markers involved in plasma membrane afferent pathways, and the endosomal/lysosomal pathway. FcγRI was stained in green (H22-FITC), all other markers in red. Panels were stained as follows: *A* was stained for calreticulin, *B* for p230 (Golgi), *C* for transferrin uptake, *D* for EEA-1, *E* for CD63, *F* for LAMP-1/CD107a. *G*, Percentage colocalization with subcellular markers was calculated using Image J as described in *Materials and Methods*. Cells from three independent experiments were quantified. ∗, Statistical significance between LAMP-1 and other markers (Student's *t* test, $p < 0.05$).

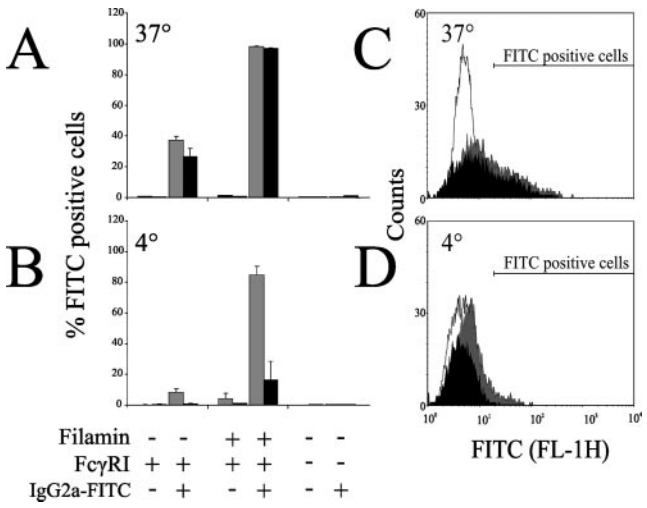

FIGURE 6. Mouse IgG2a uptake by M2 and A7 cells expressing FcγRI. Stabile clones of M2 (M2 FcγRI), A7 (A7 FcγRI), and parental M2 cells (M2) were incubated with or without mouse IgG2a-FITC for 6 h. After incubation at 37°C (*A*) or at 4°C (*B*), cells were washed at either normal pH (▨) or at pH 2.5 (■) to remove surface-bound IgG2a. Cells were analyzed by flow cytometry. Bar graphs show the percentage of FITC-positive cells defined by regions drawn in *C* and *D*. Bars represent the mean of three experiments. Error bars indicate SD. *C* and *D*, Histograms from one representative experiment of M2 cells expressing FcγRI incubated with mouse IgG2a-FITC at 37°C (*C*) or at 4°C (*D*). Open histograms represent cells without mIgG2a; gray histograms depict cells incubated with mIgG2a and washed at normal pH; black histograms represent cells washed at pH 2.5.

γ-chain (3, 4, 28). Therefore, to address whether the FcR γ-chain was capable of rescuing the impaired surface expression in this system, it was transiently cotransfected in three FcγRI-transfected M2- and A7-subcloned cell lines. No appreciable differences were observed for surface FcγRI upon mock or FcR γ-chain transfection (Fig. 4*B*, $n = 2$). FcR γ-chain transfections were confirmed by Western blot, and one representative sample is shown in Fig. 4*C*.

Next, we set out to identify the intracellular compartment in which FcγRI resides in filamin-deficient cells by immunofluorescence and electron microscopy (Fig. 5). We tested a panel of Abs recognizing compartments that are involved in afferent plasma membrane pathways such as calreticulin (Fig. 5*A*) for the ER, and p230 (Fig. 5*B*) and GM-130 (data not shown) for Golgi. Endosomal compartments were analyzed by transferrin uptake (Fig. 5*C*), and mAb stainings for EEA-1 (Fig. 5*D*), lysosomal integral membrane protein-1 (CD63; Fig. 5*E*), and lysosomal-associated membrane protein (LAMP)-1/CD107a (Fig. 5*F*). We did not observe a clearly defined compartment in which FcγRI accumulated using these markers, suggestive for a transient passage through the compartments tested. Most colocalization between FcγRI and a subcellular marker was observed for the lysosomal marker LAMP-1 as indicated by quantification of colocalized signals of cells from three different experiments (Fig. 5*G*). Treatment of cells with nocodazole, which disrupts microtubuli and disperses cellular organelles, reduced some colocalization of FcγRI and LAMP-1 (data not shown, $n = 2$). In A7 cells, intracellular FcγRI could be found in similar compartments as for cells without filamin, although A7 cells displayed plasma membrane accumulation (data not shown).

To test whether in the absence of filamin, FcγRI is indeed transported to the plasma membrane before entry into a lysosomal pathway, we performed mIgG2a-FITC capture experiments. M2 and A7 transfectants were incubated with mIgG2a-FITC at 37°C (Fig. 6, *A* and *C*) to allow binding and endocytosis or at 4°C (Fig. 6, *B* and *D*) to allow only binding to FcγRI. M2 and A7 transfectants became FITC positive after incubation with mIgG2a-FITC. Washing cells with low pH removed surface-bound IgG (Fig. 6, *B* and *C*) but only partly abrogated the FITC signal when cells were incubated at 37°C, suggesting endocytosed mIgG2a-FITC in both M2 (Fig. 6, *A* and *C*) and A7 (Fig. 6*A*) transfectants. Uptake of mIgG-FITC appeared dependent on FcγRI as the untransfected parental M2 cells did not obtain FITC signal. In combination with the colocalization experiments, these data suggested filamin to stabilize FcγRI at the plasma membrane and to prevent entry of FcγRI into a lysosomal pathway.

Total FcγRI protein levels in M2 and A7 clones were assessed by flow cytometry upon cell permeabilization with saponin (Fig. 7*A*). FcγRI protein levels were significantly reduced in the absence of filamin. To demonstrate that these cells produced significant levels of FcγRI, and that the low FcγRI amounts were a consequence of lysosomal degradation, we incubated cells with bafilomycin A1. Bafilomycin A1 inhibits the vacuolar-type H^+-ATPase

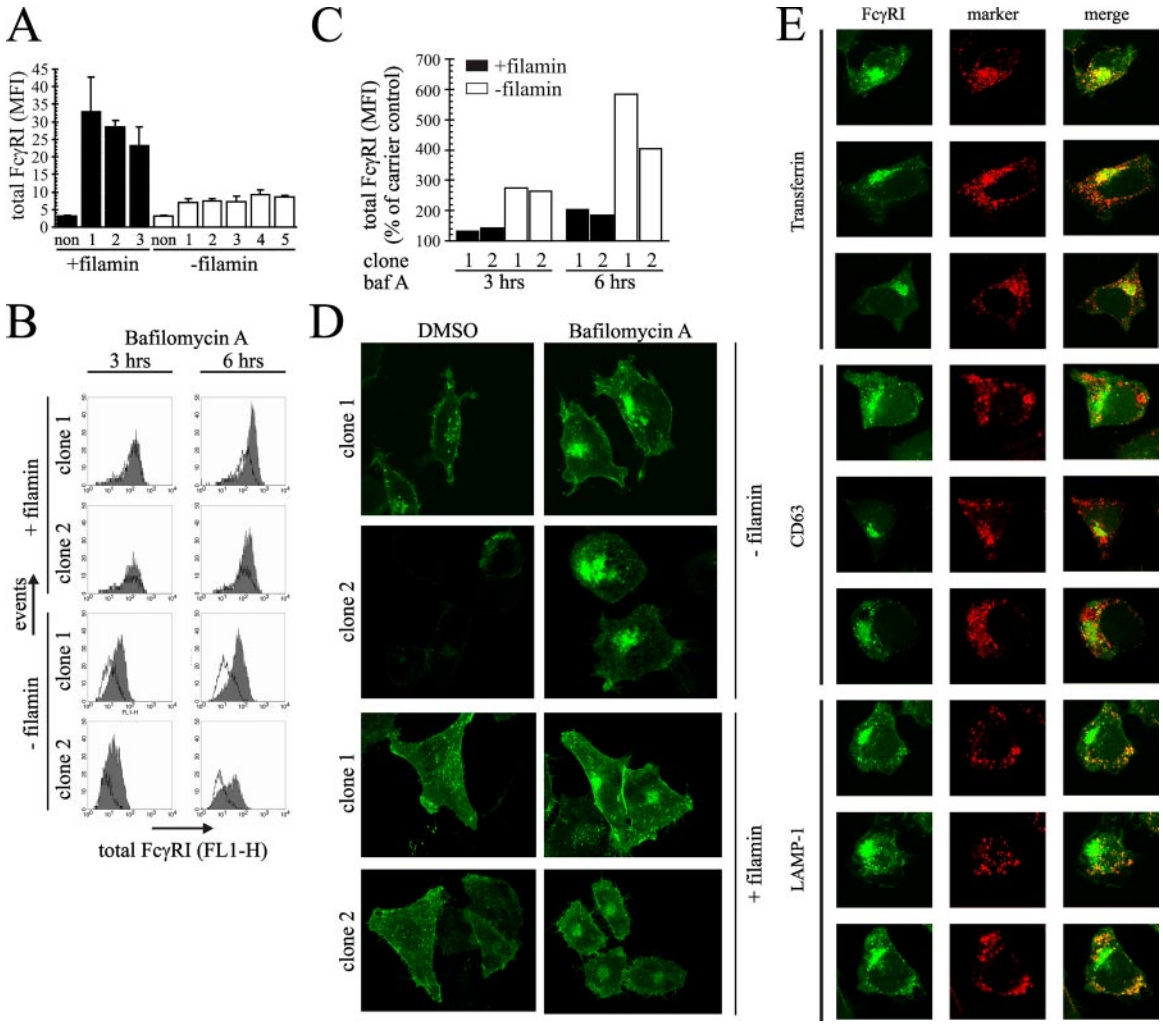

FIGURE 7. Filamin prevents lysosomal degradation of FcγRI. *A*, Filamin-positive and -negative lines that expressed FcγRI transcripts were stained for total FcγRI in the presence of 0.1% saponin. ■, A7 clones; □, M2 clones; un, untransfected cells. Numbers represent independent clones of FcγRI transfectants. Average mean values of four independent experiments are shown, error bars indicate SE, of the mean. *B*, Two FcγRI-expressing clones with or without filamin were incubated with bafilomycin A1 (100 nM) for 3 or 6 h. Total FcγRI was assessed as in *A*. Black-lined open histograms represent total FcγRI after incubation in carrier control (DMSO 500-fold diluted); gray-filled histograms represent total FcγRI after bafilomycin A1 treatment. Representative data of three independent experiments are shown. *C*, Relative increase of total FcγRI after incubation of cells with bafilomycin A1. Two FcγRI-transfected cell lines with (■) or without (□) filamin were compared. For each cell line, total FcγRI levels after DMSO incubation was set at 100%. *D*, FcγRI-transfected M2 and A7 cells were assessed by confocal microscopy after 2 h incubation with bafilomycin A1 or DMSO. FcγRI was stained by mAb 10.1 FITC-conjugated. *E*, Intracellular location of FcγRI in cells without filamin after bafilomycin A1 treatment. M2 cells were stained for markers involved in endosomal (transferrin uptake) and lysosomal (CD63, LAMP-1) pathways. FcγRI was stained in green (H22-FITC), all other markers in red.

that regulates endosomal pH, and hence prevents intracellular degradation of endocytosed cargo and receptors (35, 37). FcγRI levels in cells without filamin increased profoundly upon incubation with bafilomycin A1 (Fig. 7, *B* and *C*, $n = 3$), but not with the proteasomal inhibitor lactacystin (data not shown). After 6 h, FcγRI levels almost reached those of A7 cells incubated with carrier control. Some accumulation of FcγRI after 6 h was observed for FcγRI in A7 cells, suggesting limited lysosomal FcγRI degradation in the presence of filamin. No changes were observed for FcγRI surface levels in the presence of bafilomycin A1, suggesting FcγRI internalization not to be affected (data not shown, refs 35,37). Bafilomycin A1 clearly elevated intracellular staining of FcγRI in cells without filamin (Fig. 7*D*). Upon bafilomycin A1 treatment A7 cells showed an increase of intracellular staining of FcγRI as well (Fig. 7*D*) which coincided with flow cytometric analysis of total protein levels (Fig. 7*C*). Interestingly, bafilomycin A1 treatment caused FcγRI to accumulate predominantly in the endosomal compartment (Fig. 7*E*, transferrin staining), although some colocalization was also seen with lysosomal markers CD63 and LAMP-1.

Discussion

To identify protein effectors of FcγRI, we performed yeast two-hybrid screens and identified filamin, an actin-binding protein. This interaction was confirmed in coimmunoprecipitation experiments with endogenously expressed FcγRI and filamin (Fig. 1*B*). We found filamin to partially colocalize with FcγRI in primary monocytes after fixation (staining with mAb recognizing FcγRI, independently of bound ligand), or by addition of monomeric IgG, and an FcγRI-cross-linking mAb at 37°C before fixation (Figs. 1*C* and 2). Most colocalization was observed at the plasma membrane where filamin may act to stabilize FcγRI surface expression by tethering FcγRI to actin, and preventing FcγRI to internalize, as was suggested by our studies in filamin-deficient

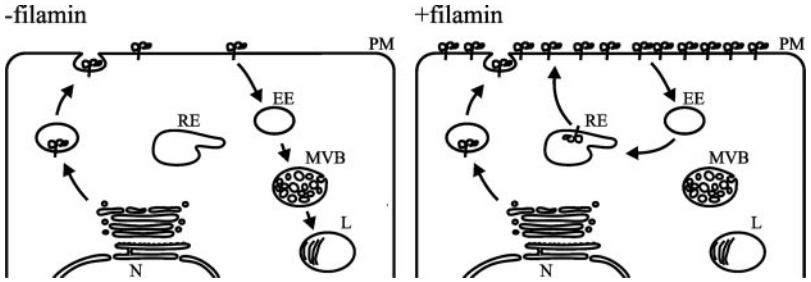

FIGURE 8. Model of FcγRI-filamin interactions. In the absence of filamin (*left panel*), FcγRI is capable of reaching the plasma membrane after synthesis, but is internalized rapidly, and routed by default toward lysosomes where it becomes degraded. In the presence of filamin (*right panel*), FcγRI is routed toward the plasma membrane after synthesis in the ER. Filamin interactions with FcγRI stabilize plasma membrane localization of FcγRI by reducing internalization of ligand-free FcγRI. Internalized FcγRI may be sequestered into a recycling pathway by filamin to further support plasma membrane expression, and prevent unwanted lysosomal degradation of receptor and cargo; EE, early endosome; L, lysosome; MVB, multivesicular body; N, nucleus; PM, plasma membrane; RE, recycling endosome.

cells. As monomeric IgG induces FcγRI internalization into a recycling route that prevents its lysosomal degradation (29), intracellular FcγRI-filamin interactions upon monomeric IgG incubation may contribute to its surface expression by retaining FcγRI in a recycling pathway, similar as described for calcitonin receptor-filamin interactions (19). Although our data suggest that IgG-occupied FcγRI can interact with filamin (Fig. 2), a previous report indicated filamin to preferentially interact with ligand-free FcγRI (11). As suggested by these authors, effective IgG-induced dissociation of FcγRI-filamin might require larger IgG complexes that may coincide with induction of phagocytosis (11).

We observed FcγRI surface expression in vitro to depend on filamin, shown in a transfection model of cells that differed by filamin expression and by RNA interference (Figs. 3–5). Routing of FcγRI toward the plasma membrane in filamin-negative cells appeared normal: FcγRI did not accumulate in compartments that are involved in afferent plasma membrane transport such as ER and Golgi, its expression was insensitive to coexpressed FcR γ-chain, and some surface expression was observed in transient transfection experiments. Moreover, capture experiments suggested transitory FcγRI surface expression (Fig. 6) in the absence of filamin. However, a significant proportion of FcγRI localization was confined to (pre)lysosomal compartments in M2 cells as apparent from confocal studies (in the absence of cross-linking ligand; Fig. 5). FcγRI protein levels were also highly sensitive to bafilomycin A1 in cells without filamin (Fig. 6). Interestingly, bafilomycin A1 treatment of M2 cells caused FcγRI to accumulate predominantly in the endosomal compartment (Fig. 7*E*). This coincides with previous publications showing that acidification is critical for fusion of yeast vacuoles (30, 31). Capture experiments and colocalization studies suggested that FcγRI does not accumulate on the cell surface, but transiently passes through this compartment to be finally degraded in lysosomal structures. FcγRI is unique among multisubunit FcR, and harbors intracellular residues that facilitate MHC class II presentation after immune complex triggering (7). This pathway may be inhibited by filamin activity in resting immune cells to facilitate FcγRI surface expression, and prevent undesired degradation and presentation of Ags (a model is presented in Fig. 8).

Previous studies have demonstrated in vitro surface expression of FcγRI, in contrast to FcγRIII and FcεRI, to be independent of coexpressed FcR γ-chain (32, 33). FcγRI lacks ER retention motifs present in the α-chains of FcγRIII and FcεRI that are masked by the FcR γ-chain to allow surface expression (33–35). This was supported by the inability of the FcR γ-chain to rescue FcγRI surface expression in our experiments (Fig. 4). In vivo, surface expression of FcγRI, FcγRIII, and FcεRI is reduced in FcR γ-chain-deficient mice, albeit FcγRI is detectable at ~20% of wild-type levels (3–5). This may indicate that in these cells the remaining FcγRI is stabilized by filamin, or that coexpressed FcR γ-chain modulates filamin activity in vivo.

We recently reported periplakin to interact with the membrane-proximal domain of FcγRI under similar conditions as described here for filamin, albeit periplakin and FcγRI did not colocalize on intracellular vesicles (10, 22). Although it remains unclear how periplakin and filamin interact in FcγRI functioning, the present data may suggest these proteins to affect separate FcγRI functions. Blockade of FcγRI-periplakin interaction by overexpressed C-terminal periplakin or blocking peptides modulated FcγRI ligand-binding capacity and downstream effector functions but not surface expression (10, 22). Both proteins can also act as a cytoskeletal-associated scaffold for signal transducers (12, 36, 37), suggesting that periplakin and filamin may coordinate different signaling pathways. The data presented here point at a vital role for filamin in FcγRI biology by stabilizing surface expression, and retention of FcγRI from a default lysosomal pathway that mediates FcγRI degradation.

Acknowledgments

We thank Drs. Y. Ohta and R. T. Miller for full-length filamin cDNA construct and yeast-two-hybrid constructs, respectively, Dr. E. van Binsbergen (Department of Medical Genetics, University Medical Center (UMC), Utrecht, The Netherlands) for help with confocal studies, and J. M. Griffith and M. J. Kleijmeer (Department of Cell Biology, UMC, Utrecht, The Netherlands) for helpful discussions.

Disclosures

The authors have no financial conflict of interest.

References

1. Ravetch, J. V., and S. Bolland. 2001. IgG Fc receptors. *Annu. Rev. Immunol.* 19: 275–290.
2. Ernst, L. K., A. M. Duchemin, and C. L. Anderson. 1993. Association of the high-affinity receptor for IgG (FcγRI) with the γ subunit of the IgE receptor. *Proc. Natl. Acad. Sci. USA* 90: 6023–6027.
3. Takai, T., M. Li, D. Sylvestre, R. Clynes, and J. V. Ravetch. 1994. FcR γ chain deletion results in pleiotrophic effector cell defects. *Cell* 76: 519–529.
4. van Vugt, M. J., A. F. Heijnen, P. J. Capel, S. Y. Park, C. Ra, T. Saito, J. S. Verbeek, and J. G. van de Winkel. 1996. FcR γ-chain is essential for both surface expression and function of human FcγRI (CD64) in vivo. *Blood* 87: 3593–3599.
5. Barnes, N., A. L. Gavin, P. S. Tan, P. Mottram, F. Koentgen, and P. M. Hogarth. 2002. FcγRI-deficient mice show multiple alterations to inflammatory and immune responses. *Immunity* 16: 379–389.
6. Ioan-Facsinay, A., S. J. de Kimpe, S. M. Hellwig, P. L. van Lent, F. M. Hofhuis, H. H. van Ojik, C. Sedlik, S. A. da Silveira, J. Gerber, Y. F. de Jong, et al. 2002. FcγRI (CD64) contributes substantially to severity of arthritis, hypersensitivity responses, and protection from bacterial infection. *Immunity* 16: 391–402.

7. van Vugt, M. J., M. J. Kleijmeer, T. Keler, I. Zeelenberg, M. A. van Dijk, J. H. Leusen, H. J. Geuze, and J. G. van de Winkel. 1999. The FcγRIa (CD64) ligand binding chain triggers major histocompatibility complex class II antigen presentation independently of its associated FcR γ-chain. *Blood* 94: 808–817.
8. Edberg, J. C., A. M. Yee, D. S. Rakshit, D. J. Chang, J. A. Gokhale, Z. K. Indik, A. D. Schreiber, and R. P. Kimberly. 1999. The cytoplasmic domain of human FcγRIa alters the functional properties of the FcγRI.γ-chain receptor complex. *J. Biol. Chem.* 274: 30328–30333.
9. Beekman, J. M., J. E. Bakema, J. G. J. van de Winkel, and J. H. W. Leusen. 2004. Direct interaction between FcγRI (CD64) and periplakin controls receptor endocytosis and ligand binding capacity. *Proc. Natl. Acad. Sci. USA* 101: 10392–10397.
10. Beekman, J. M., J. E. Bakema, J. van der Linden, B. Tops, M. Hinten, M. van Vugt, J. G. van de Winkel, and J. H. Leusen. 2004. Modulation of FcγRI (CD64) ligand binding by blocking peptides of periplakin. *J. Biol. Chem.* 279: 33875–33881.
11. Ohta, Y., T. P. Stossel, and J. H. Hartwig. 1991. Ligand-sensitive binding of actin-binding protein to immunoglobulin G Fc receptor I (Fc γ RI). *Cell* 67: 275–282.
12. Stossel, T. P., J. Condeelis, L. Cooley, J. H. Hartwig, A. Noegel, M. Schleicher, and S. S. Shapiro. 2001. Filamins as integrators of cell mechanics and signalling. *Nat. Rev. Mol. Cell Biol.* 2: 138–145.
13. van der Flier, A., and A. Sonnenberg. 2001. Structural and functional aspects of filamins. *Biochim. Biophys. Acta* 1538: 99–117.
14. Cunningham, C. C., J. B. Gorlin, D. J. Kwiatkowski, J. H. Hartwig, P. A. Janmey, H. R. Byers, and T. P. Stossel. 1992. Actin-binding protein requirement for cortical stability and efficient locomotion. *Science* 255: 325–327.
15. He, H. J., S. Kole, Y. K. Kwon, M. T. Crow, and M. Bernier. 2003. Interaction of filamin A with the insulin receptor alters insulin-dependent activation of the mitogen-activated protein kinase pathway. *J. Biol. Chem.* 278: 27096–27104.
16. Hjalm, G., R. J. MacLeod, O. Kifor, N. Chattopadhyay, and E. M. Brown. 2001. Filamin-A binds to the carboxyl-terminal tail of the calcium-sensing receptor, an interaction that participates in CaR-mediated activation of mitogen-activated protein kinase. *J. Biol. Chem.* 276: 34880–34887.
17. Lin, R., K. Karpa, N. Kabbani, P. Goldman-Rakic, and R. Levenson. 2001. Dopamine D2 and D3 receptors are linked to the actin cytoskeleton via interaction with filamin A. *Proc. Natl. Acad. Sci. USA* 98: 5258–5263.
18. Onoprishvili, I., M. L. Andria, H. K. Kramer, N. Ancevska-Taneva, J. M. Hiller, and E. J. Simon. 2003. Interaction between the mu opioid receptor and filamin A is involved in receptor regulation and trafficking. *Mol. Pharmacol.* 64: 1092–1100.
19. Seck, T., R. Baron, and W. C. Horne. 2003. Binding of filamin to the C-terminal tail of the calcitonin receptor controls recycling. *J. Biol. Chem.* 278: 10408–10416.
20. Kiema, T., Y. Lad, P. Jiang, C. L. Oxley, M. Baldassarre, K. L. Wegener, I. D. Campbell, J. Ylanne, and D. A. Calderwood. 2006. The molecular basis of filamin binding to integrins and competition with talin. *Mol. Cell* 21: 337–347.
21. Nakamura, F., R. Pudas, O. Heikkinen, P. Permi, I. Kilpelainen, A. D. Munday, J. H. Hartwig, T. P. Stossel, and J. Ylanne. 2006. The structure of the GPIb-filamin A complex. *Blood* 107: 1925–1932.
22. Beekman, J. M., J. E. Bakema, J. G. J. Van De Winkel, and J. H. W. Leusen. 2004. Direct interaction between FcγRI (CD64) and periplakin controls receptor endocytosis and ligand binding capacity. *Proc. Natl. Acad. Sci. USA* 101: 10392–10397.
23. Kessels, H. W., M. D. van Den Boom, H. Spits, E. Hooijberg, and T. N. Schumacher. 2000. Changing T cell specificity by retroviral T cell receptor display. *Proc. Natl. Acad. Sci. USA* 97: 14578–14583.
24. Shen, L., M. van Egmond, K. Siemasko, H. Gao, T. Wade, M. L. Lang, M. Clark, J. G. van De Winkel, and W. F. Wade. 2001. Presentation of ovalbumin internalized via the immunoglobulin-A Fc receptor is enhanced through Fc receptor γ-chain signaling. *Blood* 97: 205–213.
25. Vidarsson, G., A. M. Stemerding, N. M. Stapleton, S. E. Spliethoff, H. Janssen, F. E. Rebers, M. de Haas, and J. G. van de Winkel. 2006. FcRn: an IgG receptor on phagocytes with a novel role in phagocytosis. *Blood* 108: 3573–3579.
26. Heijnen, I. A., M. J. van Vugt, N. A. Fanger, R. F. Graziano, T. P. de Wit, F. M. Hofhuis, P. M. Guyre, P. J. Capel, J. S. Verbeek, and J. G. van de Winkel. 1996. Antigen targeting to myeloid-specific human FcγRI/CD64 triggers enhanced antibody responses in transgenic mice. *J. Clin. Invest.* 97: 331–338.
27. Wallace, P. K., T. Keler, K. Coleman, J. Fisher, L. Vitale, R. F. Graziano, P. M. Guyre, and M. W. Fanger. 1997. Humanized mAb H22 binds the human high affinity Fc receptor for IgG (FcγRI), blocks phagocytosis, and modulates receptor expression. *J. Leukocyte Biol.* 62: 469–479.
28. van Egmond, M., A. J. van Vuuren, H. C. Morton, A. B. van Spriel, L. Shen, F. M. Hofhuis, T. Saito, T. N. Mayadas, J. S. Verbeek, and J. G. van de Winkel. 1999. Human immunoglobulin A receptor (FcαRI, CD89) function in transgenic mice requires both FcR γ chain and CR3 (CD11b/CD18). *Blood* 93: 4387–4394.
29. Harrison, P. T., W. Davis, J. C. Norman, A. R. Hockaday, and J. M. Allen. 1994. Binding of monomeric immunoglobulin G triggers FcγRI-mediated endocytosis. *J. Biol. Chem.* 269: 24396–24402.
30. Peters, C., M. J. Bayer, S. Buhler, J. S. Andersen, M. Mann, and A. Mayer. 2001. *Trans*-complex formation by proteolipid channels in the terminal phase of membrane fusion. *Nature* 409: 581–588.
31. Ungermann, C., W. Wickner, and Z. Xu. 1999. Vacuole acidification is required for trans-SNARE pairing, LMA1 release, and homotypic fusion. *Proc. Natl. Acad. Sci. USA* 96: 11194–11199.
32. Miller, K. L., A. M. Duchemin, and C. L. Anderson. 1996. A novel role for the Fc receptor γ subunit: enhancement of FcγR ligand affinity. *J. Exp. Med.* 183: 2227–2233.
33. Kim, M. K., Z. Y. Huang, P. H. Hwang, B. A. Jones, N. Sato, S. Hunter, T. H. Kim-Han, R. G. Worth, Z. K. Indik, and A. D. Schreiber. 2003. Fcγ receptor transmembrane domains: role in cell surface expression, γ chain interaction, and phagocytosis. *Blood* 101: 4479–4484.
34. Ra, C., M. H. Jouvin, and J. P. Kinet. 1989. Complete structure of the mouse mast cell receptor for IgE (FcεRI) and surface expression of chimeric receptors (rat-mouse-human) on transfected cells. *J. Biol. Chem.* 264: 15323–15327.
35. Letourneur, F., S. Hennecke, C. Demolliere, and P. Cosson. 1995. Steric masking of a dilysine endoplasmic reticulum retention motif during assembly of the human high affinity receptor for immunoglobulin E. *J. Cell Biol.* 129: 971–978.
36. Van den Heuvel, A. P., A. M. de Vries-Smits, P. C. van Weeren, P. F. Dijkers, K. M. de Bruyn, J. A. Riedl, and B. M. Burgering. 2002. Binding of protein kinase B to the plakin family member periplakin. *J. Cell Sci.* 115: 3957–3966.
37. Feng, G. J., E. Kellett, C. A. Scorer, J. Wilde, J. H. White, and G. Milligan. 2003. Selective interactions between helix VIII of the human mu-opioid receptors and the C terminus of periplakin disrupt G protein activation. *J. Biol. Chem.* 278: 33400–33407.